New Forests (2015) 46:63–90
DOI 10.1007/s11056-014-9447-3

Time series analysis of forest carbon dynamics: recovery of *Pinus palustris* physiology following a prescribed fire

G. Starr · C. L. Staudhammer · H. W. Loescher · R. Mitchell · A. Whelan · J. K. Hiers · J. J. O'Brien

Received: 27 January 2014 / Accepted: 22 July 2014 / Published online: 31 July 2014

Abstract Frequency and intensity of fire determines the structure and regulates the function of savanna ecosystems worldwide, yet our understanding of prescribed fire impacts on carbon in these systems is rudimentary. We combined eddy covariance (EC) techniques and fuel consumption plots to examine the short-term response of longleaf pine forest carbon dynamics to one prescribed fire at the ends of an edaphic gradient (mesic and xeric sites). We also introduce novel (to the EC research community) statistical time-series approaches to quantify the drivers of carbon dynamics in these systems. We determined that our mesic site was a moderate sink of carbon (-157.7 ± 25.1 g C m^{-2} $year^{-1}$), while the xeric site was carbon neutral (5.9 ± 32.8 g C m^{-2} $year^{-1}$) during the study. The fire released 408 and 153 g C m^{-2} $year^{-1}$ for the mesic and xeric sites, respectively. When loss associated with fire was combined with net ecosystem exchange rates, both sites became moderate carbon sources for the year. Analyses of assimilation and respiration parameters (e.g., maximum photosynthesis, quantum efficiency, and daytime ecosystem respiration)

G. Starr (✉) · C. L. Staudhammer · A. Whelan
Department of Biological Sciences, University of Alabama, Tuscaloosa, AL 35487, USA
e-mail: gstarr@ua.edu

H. W. Loescher
National Ecological Observatory Network (NEON) Inc., 1635 38th St, Suite 100, Boulder, CO 80301, USA

H. W. Loescher
Institute of Arctic and Alpine Research (INSTAAR), University of Colorado, Boulder, CO 80309, USA

R. Mitchell
Jones Ecological Research Center, Newton, GA 39870, USA

J. K. Hiers
Natural Resource Section at Jackson Guard, Niceville, FL 32578, USA

J. J. O'Brien
Center for Forest Disturbance Science, USDA Forest Service, Athens, GA 30602, USA

showed a positive trend over time pre-fire and a negative trend over time post-fire for maximum ecosystem CO_2 uptake rates, and the opposite relationship for daytime ecosystem respiration rates. Within 30 days following fire, ecosystem physiological activity was statistically similar to pre-fire and appeared to be driven by the pine canopy. Our results suggest that prescribed fire (low intensity, high frequency) maintains the existing structure and function (in this case, carbon flux rates) because longleaf pine ecosystems have evolved with fire. This study, 1 year in length, provides a foundational understanding of the complex interaction between fire and carbon dynamics for longleaf pine ecosystems. Moreover, it provides a case study for applying time series analysis methods to EC data where there are complex relationships between ecosystem physiological activity and environmental drivers. However, to elicit a broader understanding of the complex interaction occurring between fire and carbon dynamics long- term studies are needed.

Keywords Longleaf pine · Net ecosystem exchange (NEE) · Ecosystem respiration (Reco) · Gross ecosystem exchange (GEE) · Prescribed fire · ARIMA models

Introduction

Present-day forest management techniques utilize prescribed fires to mimic historic, natural high frequency and low intensity disturbance regimes in Southeastern USA pine forests. Prescribed fire is the dominant source of ignition in *Pinus palustris* (longleaf pine) ecosystems. However, few studies have focused on the C dynamics of these ecosystems and their fire management (Wiedinmyer and Neff 2007) even though model simulations identify the interaction of water and fire as a key driver of C budgets (Ryan and Williams 2011). Because fire regulates the spatial and temporal patterns in ecosystem C dynamics (Wiedinmyer and Neff 2007), the feedbacks among fire, vegetation and the environment complicate these patterns (Mitchell et al. 2009). Temperatures in the historic range of longleaf are predicted to increase in the coming decades, though because of the dominance of convection as a driver of precipitation, how precipitation patterns in the region will change remain uncertain (Mitchell et al. 2014). Understanding these feedbacks is necessary to predict fire impacts on C budgets today and with future climate change scenarios (Wiedinmyer and Neff 2007).

The urgency to develop an understanding of these interactions has grown with the predictions of longer and more intense fire seasons for several parts of the world due to changing climate (IPCC 2014). Under IPCC scenarios, the estimated average area that will burn in some forests may double by the year 2050 (Balshi et al. 2009). These predictions of increased area burned, however, are chiefly associated with wildfires in boreal forests (Randerson et al. 2006). While much less is known with respect to how climate change will impact the carbon (C) dynamics of ecosystems dependent on frequent fire, such as savannas (Abrahamson and Hartnett 1990), we know the direct effect of fire results in the combustion of fuels that rapidly release CO_2 to the atmosphere. Biomass burning, both natural and anthropogenic, is often identified as a major regional source of atmospheric C, but one that is variable in both time and space (Wiedinmyer and Neff 2007). Yet, few empirical data sets have been produced that measure carbon dynamics through multiple disturbances such as fire (Girod et al. 2007) or include investigations of these processes across time and space.

Fire is also important in sustaining ecosystem function in global assessments. When fire is considered, it is often addressed uni-dimensionally and lacks interactive effects. Fire not only controls physiognomy (Bond et al. 2005) and productivity (Bond-Lamberty et al. 2007), but also the diversity in many forests (Kruger 1983). Recently, Grace et al. (2006) suggested that lengthening the fire return interval in savanna ecosystems could increase the amount of C stored globally. However, this management practice may be unsustainable since fire frequency, risk, and intensity are inversely related; thus, increasing periods between fire return interval would likely result in increased fuel loads and greater risk of intense wildfire (Girod et al. 2007). Clearly, filling scientific gaps in understanding how fire and water interactions regulate C dynamics in frequently burned ecosystems is necessary (Martin et al. 2001).

The pine grasslands of the southeastern coastal plain of the US provide an archetypical model to understand the interaction among fire, water and C dynamics. These systems are dependent on frequent fires to maintain their plant species richness (Kirkman et al. 2004). Alterations in ecosystem fire regimes or climate could lead to instability in these C pools that, in turn, result in additional C release to the atmosphere. We established a study in two longleaf pine ecosystems at the ends of an edaphic moisture gradient (mesic and xeric sites) to better understand the interactions between prescribed fire and C dynamics within these savanna ecosystems. We used eddy covariance (EC) techniques to assess the C dynamics in these two ecosystems prior to and following one prescribed fire. In this study, we hypothesized that: (1) Fire would not have a significant long lasting effect (less than 30 days) on longleaf pine ecosystem physiological activity as it relates to carbon dynamics since these systems evolved with fire. (2) Environmental variation would have a greater role in ecosystem carbon dynamics than would fire even over the 1 year duration of this study.

To test such hypotheses, we employed non-linear modeling, as well as time series methods utilizing autoregressive integrated moving average (ARIMA; Box et al. 1994) models. While time series methods are not new to the field of biology, we are unaware of other studies that use these methods with eddy covariance derived carbon fluxes. Therefore, an additional goal of this paper is to provide a case study for their use in quantifying the drivers of carbon dynamics in these systems.

Methods

Site description

The study was conducted at the Joseph Jones Ecological Research Center (JJERC) in southwestern Georgia, USA from July 1, 2008 to June 30, 2009. The JJERC is an 11,000 ha reserve located within the Lower Coastal Plain and has extensive stands of second-growth longleaf pine *(Pinus palustris* Mill) that is managed with low intensity, dormant-season prescribed fires (Mitchell et al. 1999).

We selected study sites with soils in two drainage classes falling on the ends of an edaphic gradient for longleaf pine–wiregrass ecosystems at the JJERC: (*i*) The mesic site (31.279°N, −84.532°W, 165 m.a.s.l.) occurs on an upland terrace with soil classified as Aquic Arenic Kandiudults. These soils are sandy loam over sandy clay loam or clay on nearly level slopes with a water holding capacity of 40 cm water m^{-1} soil (Mitchell et al. 1999). An argillic horizon is present within 50 cm of the soil surface. The xeric site (31.269°N, −84.479°W, 160 m.s.a.l.) occurs on an upland sand ridge with an undulating

slope of 3–4 % and a deep, sandy soil with no argillic horizon, i.e, no significant accumulation of clay is found within 300 cm of the surface. These soils are Typic Quartzipsamments with a water-holding capacity (in the upper 300 cm) of ~18 cm water m^{-1} of soil (Mitchell et al. 1999).

The mesic ecosystem is characterized by a single overstory of dominant longleaf pine, while the xeric ecosystems is dominated by open stands of longleaf pine and scrub oaks, where the co-dominant oak, turkey oak (*Quercus laevis* Walter) occurs in all the aboveground strata. Dense ground cover at all sites is dominated by perennial wiregrass (*Aristida stricta* Michx.), with numerous species of other perennial grasses and forbs also present (Goebel et al. 2001), yet leaf area index (LAI) is still rather small (0.65–1.1 and 0.22–0.39 m^2 m^{-2}, for the mesic and xeric sites respectively; Addington et al. 2006). These sites have previously been described by Mitchell et al. (1999). Longleaf pine ecosystems have evolved with very high fire frequency (every 1–3 years; Christensen 1981), when fire is suppressed for as little as 4 years the ecosystem loses biodiversity and its structure and function are altered (Way 2006). For this reason our study does not include a "control site" where fire is excluded. During this study, the xeric and the mesic sites were burned January 12 and 14, 2009, respectively. Both sites are on a 2-year burn cycle and were previously burned in winter 2007; this burn cycle falls within the natural frequency of fire for the ecosystem (Christensen 1981).

Each fire was set using backing fires on the downwind side of the management unit, moving the fire away from a downwind fire-break. Strip head fires were then set perpendicular to the wind, starting on the downwind end of the unit and moving upwind. Fires were initiated ~30–50 m apart depending on fuel patterns, local weather conditions, and fire behavior.

Eddy covariance methodology

Net ecosystem exchange of CO_2 (NEE) was measured continuously using open-path EC techniques (Ocheltree and Loescher 2007). By applying a control volume approach, NEE was estimated through a simplification of the continuity equation (Eq. 1). The vertical rate of change of mean molar CO_2 concentration and the vertical scalar flux divergence from ground level to the measurement height (z, m) are represented by integrals I and II in Eq. 1, respectively (Loescher et al. 2006a),

$$NEE = \underbrace{\int_0^z \frac{\partial \overline{\rho C}}{\partial t} \partial z}_{I} + \underbrace{\int_0^z \frac{\partial \overline{\rho C' w'}}{\partial t} \partial z}_{II} \quad (1)$$

where C is CO_2 concentration (μmol CO_2 m^{-3}) and w is the vertical wind velocity (m s^{-1}). Primes denote instantaneous fluctuation (at 10 Hz) about the mean, and overbars denote the mean over a 30 min averaging period. CO_2 is stored directly beneath the EC instrumentation and was calculated as a function of mean molar CO_2 concentration and measured height. CO_2 concentration and the vertical velocities were measured at a fixed plane above mean canopy height. CO_2 and water vapor concentration were measured with an open path infrared gas analyzer (IRGA, LI-7500, LI-COR Inc., Lincoln, NE, USA), and three dimensional windspeed and air temperature (T_{air}) were measured with a three dimensional sonic anemometer (CSAT3, Campbell Scientific, Logan, UT, USA). These sensors were installed approximately 4 m above mean canopy height at each site (34.5, and

34.9 m for the mesic and xeric sites, respectively). The sonic anemometer and the IRGA were placed approximately 0.2 m apart in order to minimize flow distortion. The optical path of the IRGA was vertically aligned to match the sampling volume of the sonic anemometer. Digital signals from the sonic anemometer and gas analyzer were collected by a datalogger (CR3000, Campbell Scientific Inc.) at 10 Hz. The IRGAs were calibrated every $\sim$30 day using a traceable standard for CO_2 (600 ppm $\pm$ 1.0 %), a dew point generator for H_2O (LI-610, LI-COR Inc.), and N_2 gas scrubbed with soda lime and Drierite, according to the protocols outlined by AmeriFlux (Loescher and Munger 2006).

Meteorological instrumentation

The datalogger that collected flux measurements also recorded: precipitation (TE525 Tipping Bucket Rain Gage, Texas Electronics Inc., Dallas, TX, USA), barometric pressure (Vaisala PTB110, Campbell Scientific, Logan, UT, USA), T_{air} and relative humidity (RH; Model HMP45C, Campbell Scientific, Logan, UT, USA), 4-component net radiation (NR01, Hukseflux Thermal Sensors, Delft, The Netherlands), photosynthetically active radiation (PAR; LI-190, LI-COR Biosciences, Lincoln, NE, USA), global radiation (LI-200, LI-COR Biosciences, Lincoln, NE, USA), and wind direction and velocity (Model 05103-5, R.M. Young Company Inc., Traverse City, MI, USA). Vapor pressure deficit (VPD) was calculated using the Clausius–Clapeyron equation as a function of T_{air}. Meteorological instrumentation was mounted atop the same flux towers.

Soil meteorological measurements were collected on a second datalogger (CR10X, Campbell Scientific Inc., Logan, UT, USA) and included: soil heat flux plates buried at 8 cm (HFP01, Hukseflux Thermal Sensors, Delft, The Netherlands), volumetric water content (VWC) integrated over the top 30 cm of soil (CS616 water content reflectometer, Campbell Scientific, Logan, UT, USA) and soil temperature at 4 and 8 cm below the soil surface (Type-T copper—constantan thermocouples, Omega Engineering, Inc., Stamford, CT, USA). All sensors were measured every 10 s and averaged every 30-min.

Data processing

Raw EC data were processed using EdiRe (v.1.4.3.1184; Clement 1999), which carried out a 2-d coordinate rotation of the horizontal wind velocities to obtain turbulence statistics perpendicular to the local streamline. The covariance between turbulence and scalar concentrations was maximized through the examination of the time series at 0.1 s intervals on both sides of a fixed lagtime (in this case, $\pm$0.3 s) following Loescher et al. (2006b). Using this approach, we found that the 2-d rotation minimized uncertainty from one 30-min average to another due to the definition of the coordinate framework (data not shown), and the block averaging optimized the range of turbulent frequencies captured. In addition the study areas have relatively short roughness lengths (0.75 m), uniform canopy structure ($\sim$22.0 and 23.0 m canopy height for the xeric and mesic, respectively), and relatively flat topography (<0.5 m of elevation change within each towers footprint). Because of this we assumed that the influence of coherent structures (i.e., ramp structures, Loescher et al. 2006b) and low frequency effects were captured by this approach. Fluxes were calculated for half-hour intervals and then corrected for the mass transfer resulting from changes in density not accounted for by the IRGA (Massman 2004), and differences in the frequency response between the CSAT3 and the Li-7500 (Massman 2000). Barometric pressure data were used to pressure correct all fluxes.

Flux data screening was applied following to eliminate 30-min fluxes resulting from systematic errors such as: (1) rain and condensation in the sampling path as indicated by an automatic gain control value >62 (Li-7500 Li-Cor Manual), (2) incomplete 30-min datasets during system calibration or maintenance, (3) values of the standard deviations for *u, v*, and *w* winds greater than 3.0, (4) CO_2 concentration outside feasible range, and, (5) poor coupling of the canopy with the external atmospheric conditions, as defined by the friction velocity, u*, using a threshold <0.20 m s^{-1} (Whelan et al. 2013). Because these pine ecosystems have an open and evergreen canopy, with little seasonal structure change, seasonal differences in the u* threshold were not observed (data not shown). Quality assurance of the flux data was also maintained by examining plausibility tests (i.e., NEE <−30 and NEE >30 μmol m^{-2} s^{-1}), stationarity criteria, and integral turbulent statistics (Foken and Leclerc 2004).

EC measurements of NEE were estimated at a temporal resolution of 30 min (Loescher et al. 2006a), such that:

$$\mathrm{NEP} \approx -\mathrm{NEE} \tag{2a}$$

$$\mathrm{GPP} \approx \mathrm{GEE} = -\mathrm{NEE} + \mathrm{R_{eco}} \tag{2b}$$

where, NEP is net ecosystem production, GPP is gross primary production, GEE is gross ecosystem exchange, and R_{eco} is ecosystem respiration. GPP cannot be measured directly using standard eddy covariance techniques, but rather is estimated from the right hand terms in Eq. 2b. Half hourly fluxes of NEE (μmol m^{-2} s^{-1}) were used to calculate GEE in g C m^{-2} s^{-1} from Eqs. 2a, 2b, which follow the logic that govern productivity in Randerson et al. (2002) and that govern the interpretation of those processes using the micrometeorological measurement approaches in Loescher et al. (2006a).

Missing half hourly data were gap-filled using separate functions for day and night (NEE_{day}, NEE_{night}). We used the functional forms of the Michaelis–Menten (Ruimy et al. 1995) and Lloyd and Taylor (1994) equations for our data for day and night gap-filling, respectively. When PAR was ≥10 μmol m^{-2} s^{-1}, NEE data were gap-filled with Eq. 3, and when PAR was <10 μmol m^{-2} s^{-1}, NEE data were gap-filled using Eq. 4:

$$NEE_{day} = \frac{\alpha\phi P_{\max}}{\alpha\phi + P_{\max}} + R_d \tag{3}$$

$$NEE_{night} \approx \mathrm{R}_{eco} = R_0 e^{bT_{air}} \tag{4}$$

where, α is the apparent quantum efficiency (−μmol CO_2 μmol $quanta^{-1}$), ϕ is PAR (μmol quanta), R_d is ecosystem respiration (μmol CO_2 m^{-2} s^{-1}), P_{max} is the maximum ecosystem CO_2 uptake rate (μmol CO_2 m^{-2} s^{-1}), R_0 is the base respiration rate when air temperature is 0 °C, and *b* is an empirical coefficient. These functional relationships were calculated on a monthly basis by site to gap-fill where enough data were available. When too few observations were available to produce stable and biologically reasonable parameter estimates, equations estimated from annual data were used to gap-fill data by site.

Half hourly NEE, GEE, and R_{eco} values were used to generate summed pre-and post-fire, and annual descriptive statistics. Gap-filled data accounted for 28 and 37 % of daytime and 55 and 65 % of nighttime values for mesic and xeric sites, respectively.

Error estimation from gap-filled values of NEE was performed via bootstrap methods (Whelan et al. 2013). We generated 1,000 synthetic datasets for each estimated gap-filling model (day and night models in Eqs. (3) and (4), respectively), and constructed the distribution of each model parameter. Bootstrap procedures were performed monthly for gap-

filling models to estimate missing NEE_{day} data, and for 16 of the 24 months for estimating missing NEE_{night} data. The remaining 8 months utilized annual NEE_{night} equations from their respective sites. In all cases, parameter estimates from the original data were biologically reasonable and within the 95 % confidence region constructed from the bootstrap samples (Tables 5 and 6 in Appendix).

Fuel consumption

Due to the fast movement of the prescribed fire, the 30 m NEE data products showed no evidence of elevated CO_2 concentrations or variation in fluxes; therefore we account for loss of carbon by combining annual EC estimates of NEE and biomass consumption estimates. Carbon loss from prescribed burning was measured using the methods described by Ottmar et al. (2007). Destructive harvest of herbaceous fuels, litter and any woody plants <1 m in height were collected from 0.75 m^2 circular plots. The number of plots was determined based on the variability among plots, such that the standard error of mean (SEM) was <15 % of the mean value. The number of samples varied from 10 to 20 by site to maintain 15 % SEM. Post-fire fuel assessments were made within 3 days of fire to collect any unburned organic matter in the same categories as above but using 2 m × 2 m plots. Consumption was determined by subtracting post-burn biomass from pre-burn estimates. Samples were dried at 70 °C for a minimum of 48 h, then mass was recorded. The amount of carbon was assumed to be 50 % of the dry weight of organic matter.

Tree mortality

Within the footprint of each flux tower we established 4 monitoring plots (50 × 50 m) in which we recorded the location and size of all trees with diameter at breast height (DBH) over 5 cm. Each tree was assessed at the end of the growing season, November 2008. The following November all trees were again surveyed to determine mortality. If a tree was classified as dead, we assessed the cause of mortality (i.e. fire, lightning or insect infestation). This survey was conducted to provide evidence that the prescribed fire had a negligible effect on forest canopy cover and ultimately the ecosystem's physiology.

Statistical analysis

Statistical models were formulated to test hypotheses about relationship between pre- and post-fire CO_2 exchange, and environmental drivers of CO_2 exchange. All analyses were conducted using SAS software (Version 9.2; SAS Institute Inc., Cary, NC, USA). To evaluate the recovery in physiological activity following prescribed fire (hypothesis 1), we investigated NEE light response and temperature response curves (Eqs. 3 and 4, respectively). Curves were fit separately for each day to characterize changes in the response curves at time points moving from pre- to post-fire. Curves were fit using the SAS procedure PROC NLIN using data from days where there were at least ten non-missing (i.e., non-gap-filled) observations. In order to characterize changes in the shape and asymptotic behavior of the curve, the estimated parameters α, P_{max}, R_d, R_0, and b were used as response variables in five separate general linear models (GLMs). The SAS procedure PROC GLM was used to estimate the effects of site, day, and pre-/post-burn on the light and temperature response curve parameters. Residuals were tested to ensure that they met the assumption of independence via the Durbin–Watson autocorrelation test, as well as

normality and homoscedasticity. Least square mean estimates of the curve parameters were then used to graph results and to better visualize the temporal effect of fire on NEE's light and temperature response.

To test hypothesis (2), ARIMA models were formulated for NEE and R_{eco}. Since half-hourly flux data contain high levels of autocorrelation, simpler methods, such as general linear models (GLMs) cannot be used, as data violate the assumption of independence and the resultant tests of significance are far more sensitive than ecologically or statistically appropriate. To mitigate issues of autocorrelation, some previous studies have utilized summary data to formulate GLMs (Whelan et al. 2013). Data summarization, however, greatly reduces the number of time points available for analysis, and may introduce bias as a consequence of Jensen's inequality (Sierra et al. 2009). The advantage of using ARIMA models is that the internal structure of the data (e.g., autocorrelation, seasonality) is explicitly accounted for by incorporating past values, and the complete record of observations can be used. For example, a first-order autoregressive moving average, or ARMA(1,1) model, predicts the current time period value (Y_t) using its one period previous value (Y_{t-1}) and its associated error (ε_{t-1}):

$$Y_t = \mu + \alpha_1 Y_{t-1} + \varepsilon_t + \theta\varepsilon_{t-1} \tag{5}$$

where μ is the mean of the series, α_1 is the first-order autoregressive (AR) coefficient, ε is the first-order moving average (MA) coefficient, ε_t is the current period error, and ε_{t-1} is its one period previous error. A diurnal component can be added to the model by adding "seasonal effects" lagged every 48 observations (equivalent to 1 day). Potential covariates ($\mathbf{X}$) can also be added as predictor variables, which may also have lagged components:

$$Y_t = \mu + \alpha_1 Y_{t-1} + \alpha_{48} Y_{t-48} + \mathbf{X}\beta + \varepsilon_t + \theta\varepsilon_{t-1} \tag{6}$$

where α_{48} is the AR coefficient associated with a lag of 48 periods (1 day), Y_{t-48} is the observation taken at that period, and $\boldsymbol{\beta}$ is a vector of coefficients associated with each covariate.

Since these models are adversely affected by missing data, gap-filled NEE and R_{eco} data were employed. To appropriately account for uncertainty in gap-filled predictions, the estimated random error associated with prediction equations was included in each prediction. Environmental variables investigated as explanatory variables included PAR, net radiation, wind speed and direction, precipitation, T_{air}, RH, atmospheric pressure, VWC, T_{soil}, and VPD. A correlation analysis was first employed to investigate relationships among and between explanatory and response variables in order to better formulate subsequent models (results not shown). Since RH and net radiation exhibited extremely high correlations with VPD and PAR, respectively, they were dropped from further analyses to avoid multicollinearity issues.

Following Brocklebank and Dickey (2003), all data series were first investigated for stationarity, "pre-whitened" to white noise, and each independent variable's cross-correlation functions (CCF) with each response was examined to quantify lagged relationships. Strictly stationary processes are those where the mean and standard deviation do not change over time. We utilized the SAS procedure PROC ARIMA, verifying stationarity via the augmented Dickey–Fuller test (Dickey and Fuller 1979). While the usual Pearson correlation coefficient measures the synchronous correlation between two data series, the CCF measures the asynchronous similarity between two series as time is lagged between them. The CCF was computed for each input series with each response variable; however, if an input series is autocorrelated, CCFs can be misleading. Thus, ARIMA models were

identified for each input series utilizing the smallest canonical correlation method, and series the residual, pre-whitened series were used in computing each CCF (Box et al. 1994). Graphical representations of each series' correlation function were further used to identify cyclical (daily) lags using a window of 10 days. We generated CCFs over a range of positive and negative time lags to determine the time-dependent nature of relationships between the dependent variables (NEE and R_{eco}) and each pre-whitened input variable.

A full model including all environmental variables and their interactions with fire was first estimated via the SAS procedure PROC ARIMA, and appropriate AR and MA components were retained by examining autocorrelation patterns of model residuals. Model fit was evaluated via Akaike's Information Criteria (AIC). Non-significant effects ($p < 0.05$) were dropped sequentially from models until all effects remaining were significant and/or no AIC improvements were made. Residuals from final estimated models were tested for normality, homoscedasticity, and autocorrelation. Models of NEE and R_{eco} as a function of burning and environmental variables were estimated by site, and a Bonferroni correction was used to compare the effects of environmental variables and fire between sites.

Results

Environmental conditions

Though the mesic and xeric sites differ markedly in soil water holding capacity, they are separated spatially by less than 5 km, and thus most of the other environmental variables are quite similar between sites (Fig. 1). Over the study period, the lowest monthly mean temperature occurred during January 2009 (10.7 °C at both sites), and the highest monthly mean temperature occurred in June 2009 (27.4 and 27.6 °C at the mesic and xeric sites, respectively). The long term mean temperatures for the coldest and warmest months are 9.6 and 26.2 °C (NCDC 2002, Station ID: COOP 090140). The mean annual temperature at both sites, as well as the long-term mean annual temperature for the area was 19.1 °C (NCDC 2002, Station ID: COOP 090140). Similar to PAR, both VPD and RH roughly followed seasonal patterns, and differed little between the two sites (Fig. 1). The lowest values occurred during the winter months and higher values occurred during the warmer summer months (Fig. 1d, e). There were some small differences (<5 mm $month^{-1}$) in precipitation totals between the xeric and mesic sites, mostly due to local convective-driven precipitation, as opposed to synoptic-scale events (Fig. 1b). Over the measurement period, precipitation totaled 1,365 mm at the xeric site and 1,429 mm at the mesic site. These totals were slightly higher than the long-term mean total annual precipitation for the area of 1,343 mm (NCDC 2002). Because sites were chosen by differences in soil water holding capacity, there were noticeable and expected differences in VWC. In general, the xeric site had lower VWC over the measurement period than that found at the mesic site (Fig. 1c). One exception to this difference was in the late summer and fall of 2008, when there was virtually no difference in VWC (Fig. 1c). Lastly, the sites differed markedly in wind patterns, with the xeric site experiencing about 10 % higher wind speeds.

Annual carbon balance and fire

The annual NEE measured via EC methods in the mesic site was -157.7 ± 25.1 g C m^{-2} $year^{-1}$, making it a moderate carbon sink during the course of this study, while the annual

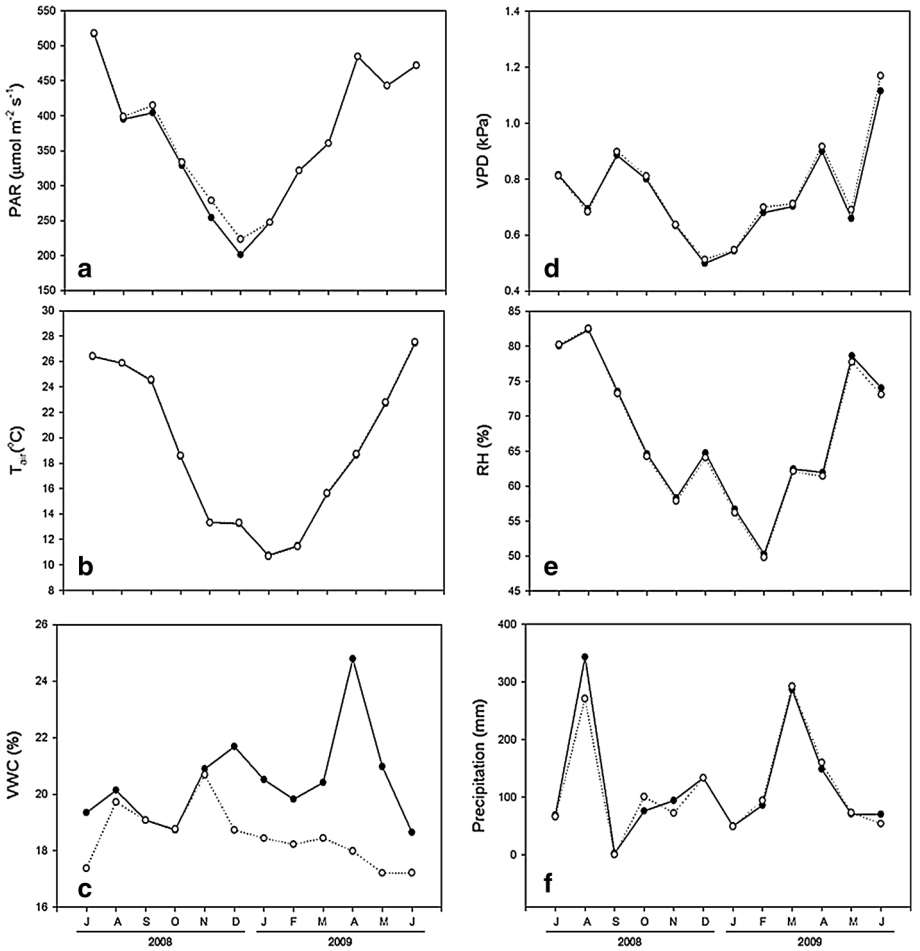

Fig. 1 Environmental variables measured at mesic and xeric sites at the Jones Center from July 2008 to June 2009. Monthly means were calculated for: **a** photosynthetically active radiation (PAR), **b** air temperature (T_{air}), **c** volumetric water content (VWC), **d** vapor pressure deficit (VPD), **e** relative humidity (RH). Monthly sums were calculated for precipitation (**f**). *Open dots and filled dots* represent data from the xeric and mesic sites, respectively. Prescribe fires were conducted in January of 2009 at both of the sites

estimate for NEE in the xeric site suggested it was carbon neutral (5.9 ± 32.8 g C m^{-2} $year^{-1}$) (Table 1). Carbon loss from fuel consumption by the fire was estimated from clip plots as 407.6 and 152.6 g C m^{-2} for the mesic and xeric sites, respectively. Litter accounted ~82 % of the carbon lost on consumption from each site, ~9 and 6 % of the loss could be attributed to pine cones at the xeric and mesic sites, respectively. The remaining losses on ignitions could be contributed to coarse woody material consumption (3 and 9 % for the xeric and mesic sites, respectively), ~0.5 and 2 % for grasses at the xeric and mesic sites, respectively). The small remaining losses were attributed to woody shrubs (<1 % at each site). When the carbon losses associated with fire were combined with our annual NEE rates, both sites were carbon sources, with the mesic site releasing 249.9 and the xeric site 163.9 C m^{-2} $year^{-1}$, respectively during the study period.

The survey of tree mortality post-fire showed a total of 3 trees died the year following fire (two at the xeric and one at the mesic sites). In both cases visual inspection showed that these trees were killed by lightning, not prescribed fire. This equates to <1 tree per hectare and in each case the tree was a mid-story individual and had no substantial effect on the carbon dynamics of the ecosystem.

Fire effects on NEE_{day}

NEE_{day} (Eq. 3) was modeled on a daily basis by site for all days where less than 50 % of values were gap-filled, resulting in 565 curves (301 and 264 from the mesic and xeric sites, respectively). More than half of the curves were fit with >21 observations, and less than 1 % of the curves had fewer than 11 observations. Curve fits which produced statistical or biologically infeasible results were discarded, resulting in parameter estimates from 397 days (217 and 180 from the mesic and xeric sites respectively).

GLMs of the parameter estimates for the light response curve (α, P_{max}, and R_d) were estimated, and in all cases the Durbin–Watson statistic indicated that data met the independence assumption for GLM. The interactions of burn (pre- vs. post-), site, and day number were added to the model with simple effects to enable different linear effects pre- and post-burn in each site. A quadratic effect for day number was also added to the model to accommodate the peaking curvilinear relationships of the parameters versus day, which were apparent from initial exploratory plots of the data. Results indicated that α, P_{max}, and R_d were significantly different over site, burn, and day number, and the significant quadratic effect of day indicated that the effects over time were non-linear (Table 2), though results for R_d were only marginally significant ($0.05 < p < 0.10$).

Apparent quantum efficiency (α) was significantly different by site pre-burn, with lower values at the mesic site ($p = 0.011$); however, values were virtually identical by site post-burn (Fig. 2a). α values also showed a curvilinear trend over time ($p < 0.001$), peaking at ~December 1, 2008 and dipping to a substantially lower value in both sites in June 2009, indicating that the apparent quantum efficiency was lower 6 months post-burn versus 6 months pre-burn.

Table 1 Annual (g C m^{-2} $year^{-1}$) and pre/post-fire estimates (g C m^{-2} $season^{-1}$) of net ecosystem exchange (NEE), gross ecosystem exchange (GEE), and ecosystem respiration (R_{eco}) for the mesic and xeric sites

Site	NEE	R_{eco}	GEE	R_{eco}/GEE (%)
Mesic				
Pre-fire	−33.2 ± 14.8	901.9 ± 14	935.1 ± 20.8	96.5 ± 3.7
Post-fire	−124.5 ± 10.3	700.9 ± 11.2	824.4 ± 15.4	85 ± 3
Year total	−157.7 ± 25.1	1,602.8 ± 25.1	1,759.4 ± 36.2	91.1 ± 3.4
Xeric				
Pre-fire	−5.4 ± 20.4	865.3 ± 14.2	870.9 ± 25.1	99.4 ± 4.6
Post-fire	11.3 ± 12.4	686.2 ± 11.7	674.9 ± 16.8	101.7 ± 4.4
Year total	5.9 ± 32.8	1,551.5 ± 25.9	1,545.7 ± 42	100.4 ± 4.5

Estimates reported in this table do not include the estimated C emissions from combustion during the fires. Convention follows Eq. 2a, 2b.

Table 2 Tests of fixed effects for models of light response curve parameters for apparent quantum efficiency, maximum ecosystem CO_2 uptake rate, and ecosystem respiration (α, P_{max}, and R_d, respectively; Eq. 3) as a function of site, pre- versus post-burn, and day number and its square

Effect	Num DF	α (μmol CO_2 μmol quanta^{-1})			P_{max} (μmol CO_2 m^{-2} s^{-1})			R_d (μmol CO_2 m^{-2} s^{-1})		
		Den DF	F value	Pr > F	Den DF	F value	Pr > F	DenDF	F value	Pr > F
Day number	1	391	24.18	<0.001	387	6.59	0.011	388	0.8	0.371
Day number^2	1	391	51.15	<0.001	387	5.27	0.022	388	1.43	0.232
Site	1	391	1.97	0.161	387	8.69	0.003	388	0.02	0.889
Day × site	1				387	0.22	0.641	388	0.21	0.644
Burn	1	391	13.27	<0.001	387	26.75	<0.001	388	1.91	0.168
Day × burn	1				387	24.92	<0.001	388	1.68	0.196
Site × burn	1	391	6.59	0.011	387	10.32	0.001	388	3.54	0.061
Day × site × burn	1				387	10.66	0.001	388	2.73	0.099

The NEE averaging period of this analysis is 0.5 h

Num DF numerator degrees of freedom for F test, *Den DF* denominator degrees of freedom for F test

P_{max} values (which represent maximum ecosystem CO_2 uptake rate) decreased over time at both sites from summer to winter up to the time of the burn, and then increased after the burn (Fig. 2b). The two sites were significantly different during the 3 months leading up to the burn, and after the burn until May 2009. A stronger quadratic effect of day in the mesic site indicated a dampened response of P_{max} values as compared that in the xeric site. While the transition at the mesic site from pre-burn to post-burn was almost continuous, there was an abrupt reduction in P_{max} values at the time of burn in the xeric site. Values in the mesic site for June 2009 were significantly higher versus July 2008, indicating that maximum ecosystem CO_2 uptake rate was higher 6 months post-burn versus 6 months pre-burn at the mesic site (Fig. 2b; Table 1).

R_d values decreased in both sites up to the time of the burn from summer to winter, and values at the mesic site from August through November were marginally significantly higher compared to those of the xeric site (Fig. 2c). After the burn, values of R_d increased, and values at the xeric site were higher, but not significantly so. In contrast to the results for P_{max}, a stronger quadratic effect of day in the xeric site indicated a dampened response of R_d values as compared that in the mesic site. While the transition of R_d in the xeric site from pre- to post-fire was relatively smooth, R_d at the mesic site showed an abrupt, though non-significant reduction from pre- to post-burn conditions. Immediately after the burn, R_d values at the two sites were not significantly different. R_d values in the xeric site at June 2009 were substantially higher versus July 2008, indicating that the daytime ecosystem respiration was higher 6 months post-burn versus 6 months pre-burn.

Least square means of the parameter estimates for the light response curve (α, P_{max}, and R_d) were generated for each site pre-and post-burn at various times in order to facilitate comparisons. That is, the resulting least square mean combinations of α, P_{max}, and R_d were used to generate predicted light response curves before and after burning by site (Fig. 3a, b). Post burn, the light response curve gradually shifted downward, indicating higher ecosystem uptake of C for both sites. Similar light-response curves (PAR values >150 μmol m^{-2} s^{-1}) for the xeric site and mesic site at the beginning and end of the study (190 days pre- and 160 post-burn, respectively) suggest complete recovery in the sites'

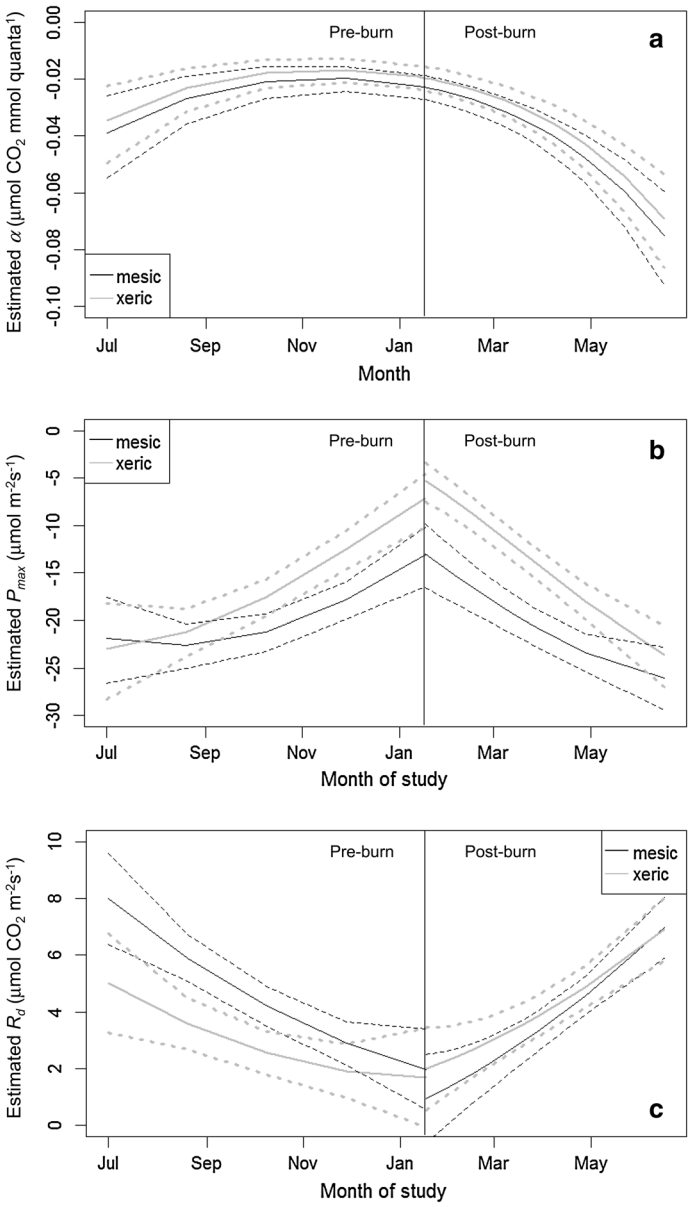

Fig. 2 Least square mean values by site pre- and post-burn over time for **a** apparent quantum efficiency (α), **b** maximum ecosystem CO_2 uptake rate (P_{max}), and **c** ecosystem respiration (R_d). 95 % confidence intervals are shown as *dotted lines*

ability to sequester carbon as a function of light (Fig. 3a, b). There were no significant differences between light response curves at the beginning and end of the study, except for high (>800) PAR values in the mesic site. Because these curves include seasonal effects as well, these results show the combined effect of seasonal changes in micrometerological

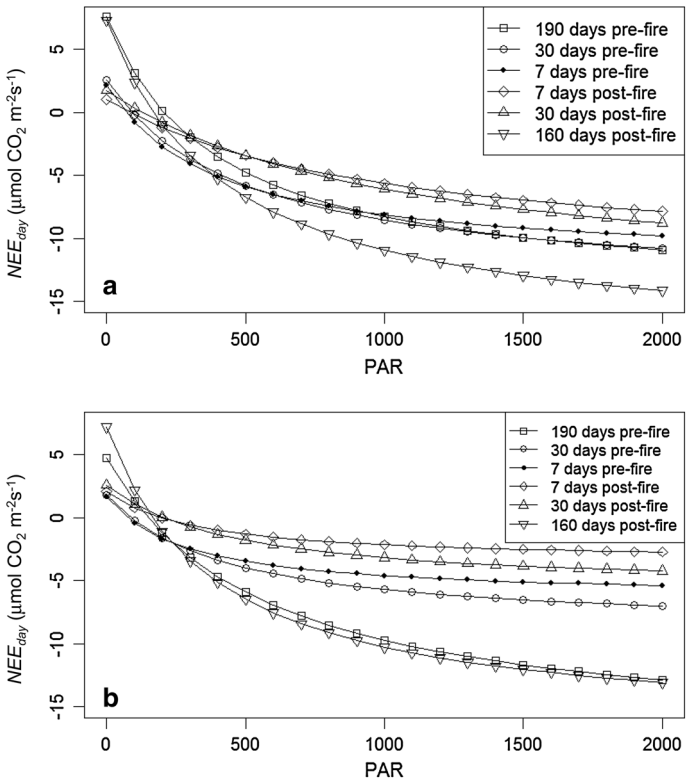

Fig. 3 Predicted light response curves for **a** mesic site and **b** xeric site, generated pre- and post-burn. Day 0 corresponds to July 1, 2008, and burn took place on Day 199

effects and that of fire. The light response curves were not significantly different in either site comparing 7 and 30 days post-fire (Fig. 3). After 30 days, the curves shift downward, which showed increased carbon uptake capacity at each site. This suggests that the effects of fire were temporary, with the influence of fire most pronounced in the 30 days post-fire.

Fire effects on NEE_{night}

GLMs of the parameter estimates for the temperature response curve (Eq. 4, R_0 and b) were estimated with fewer observations than with daytime light response curves due to the high amount of nighttime data that had to be gap-filled. Only 171 dates (94 from mesic site and 77 from xeric site) were <50 % gap-filled with stable and biologically reasonable parameter estimates. As with the light response analysis, the interactions of burn, site, and day number were added to the model with simple effects to enable different linear effects to be estimated pre-and post-burn in each site. A quadratic effect for day number was also added to the model to accommodate the curvilinear relationships of the parameters over time apparent in the data. Results indicate that only the effect of day (quadratic) was significant for R_0 ($p = 0.04$; data not shown). Values of R_0 increased up to the time of the burn, then decreased, indicating that the base respiration rate decreased following burn, and

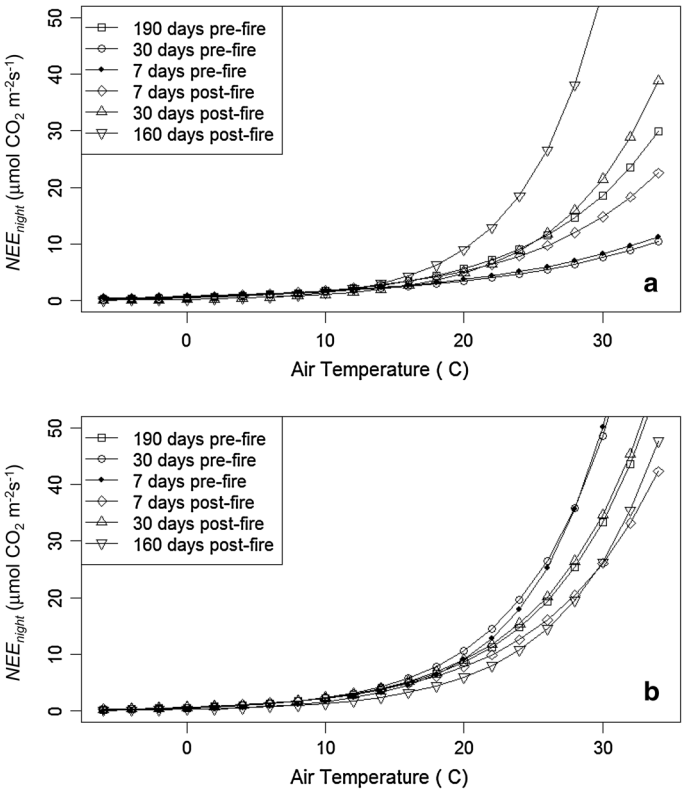

Fig. 4 Predicted temperature response curves for **a** mesic site and **b** xeric site, generated pre- and post-burn. Day 0 corresponds to July 1, 2008, and burn took place on Day 199

was lower (though not significantly so) in June 2009 versus July 2008. There were no significant differences for any effect for the empirical parameter, b ($p > 0.20$).

Similar to the light response curves, least square means of the parameter estimates for the temperature response curve parameters (R_0 and b) were generated for each site at various dates pre-and post-burn to facilitate comparisons. Although not significant, the predicted temperature response curves shifted abruptly after the burn and in a different direction in each site (Fig. 4a, b). In the mesic site, the temperature response curve shifted downward, indicating an extremely attenuated NEE_{night} response to T_{air}, whereas in the xeric site the curve shifted upward, indicating an amplified NEE_{night} response to T_{air}. Post burn, the temperature response curve gradually moved upward (less efflux) in the mesic site, recovering to its pre-burn pattern about 4 months post-burn. The response curve in the mesic site for June 2009 was much higher than that of July 2008 for temperatures above 15 °C, indicating an increased NEE response at higher temperatures. In the xeric site, the curve recovered to its pre-burn pattern within 40-days after the burn. At the end of the 1 year period of measurement, the June 2009 xeric temperature response curve was extremely attenuated versus the July 2008 measurement, indicating much less of an NEE response to temperatures above 15 °C 6 months post-fire versus 6 months pre-fire. Though our analysis of the nighttime temperature response curves lacked the statistical power to show significant differences between sites or pre- versus post-burn, these results suggest

that the burnt detritus pools and reduction in live ground cover contributed to the overall respiration budget at short timescales (<1 day^{-1}).

Interactions between fire and carbon fluxes

All series required short-term lags of ½- and 1-h for pre-whitening prior to estimating models of NEE and R_{eco}. Wind speed, rainfall, and VWC required additional 1½- and 2-h lags, VPD and pressure indicated an additional daily lag, and PAR, and T_{air} required 1- through 5-day lags. After pre-whitening, some small (<0.05) but statistically significant autocorrelation remained in pre-whitened series; however, this sensitivity resulted from the large number of observations available and was judged to be biologically insignificant. Initial cross-correlation analyses indicated small (CCF <0.10) but significant asynchronous correlations between NEE and all input variables except rainfall at half-hourly timesteps (i.e., one-period lags). There were also small, significant correlations between R_{eco} and wind speed at a half-hourly lag. This necessitated the inclusion of additional lagged autoregressive (AR) terms for these variables as predictors in ARIMA models. The autocorrelation and partial autocorrelation functions of the residuals for the models of NEE and R_{eco} indicated significant correlation patterns, which violate assumptions for testing. However, these issues were alleviated by including ½- and 1 h AR terms (one- and two-period lags, AR(1) and AR(2), respectively) and at a lag of 1 day (48 periods, AR(48)), and ½- and 1 h MA (MA(1) and MA(2), respectively) terms for the response variables themselves.

The final form of the NEE ARIMA model indicated that several independent variables had significant lagged effects at the half-hour time scale, but in all but one case the lagged effects were of similar size and direction as that of the synchronous variable. For PAR, however, the lagged effect was opposite, reducing the coincident effect by a small amount. Based on the results of the light and temperature response curve analysis (hypothesis 1), fire was included as an abrupt, temporary intervention lasting 30 days. This temporary (30 day) effect was significant and interacted with air temperature (Table 3; $p < 0.001$). While there was more uptake with increased T_{air}, the magnitude of this effect was lessened in the 30 days post-fire. In both the mesic and xeric sites, there was significantly more uptake with increased PAR, and comparison of Bonferroni corrected means indicated that uptake was significantly higher in the mesic site. On the other hand, there was significantly more uptake with increased VWC, but only in the xeric site. The ARIMA model indicated that there was significantly less uptake with increased rainfall in both sites. The Bonferroni adjustment indicated that the effects of VPD and pressure were significantly different in the mesic versus xeric sites; there was significantly less-uptake with higher VPD and significantly less uptake with higher pressure in the mesic site. These effects were not significant in the xeric site.

While lag 2 (1 h) MA and AR parameters for R_{eco} in the xeric site were not significant, removing these terms from our statistical model resulted in a higher AIC; thus these terms remained in the models for both sites. In both sites, the final estimated model for R_{eco} indicated that there was significantly less carbon release with increased atmospheric pressure (Table 4), but that this trend was reversed in the 30 days post-burn. Though this effect was not significant in the mesic site, removing it from the model resulted in a substantially higher AIC, and it was therefore retained in the model. There was significantly more carbon release with increased VPD and T_{air} ($p < 0.05$; Table 4). This trend was dampened in the 30 days post-burn, with a significant sign reversal for VPD in the mesic site. There were small, but significant effects of PAR on release of CO_2 in both the

Table 3 Parameter estimates from ARIMA model of net ecosystem exchange (NEE) by site

Parameter	Mesic site				Xeric site			
	Estimate	Standard error	t Value	Approx >|t|	Estimate	Standard error	t Value	Approx >|t|
Intercept	37.83	11.192	3.38	0.001	45.82	18.909	2.42	0.015
MA(1)	0.874	0.044	20.01	<0.0001	0.831	0.044	18.76	<0.0001
MA(2)	−0.236	0.028	−8.43	<0.0001	−0.244	0.028	−8.80	<0.0001
AR(1)	1.094	0.044	25.08	<0.0001	1.047	0.045	23.39	<0.0001
AR(2)	−0.300	0.036	−8.36	<0.0001	−0.259	0.037	−6.97	<0.0001
AR(48)	0.127	0.007	19.15	<0.0001	0.134	0.007	19.71	<0.0001
Burn	1.442	0.560	2.57	0.010	0.684	0.545	1.25	0.210
PAR	−0.005	2.3E−04	−24.1	<0.0001*	−0.004	2.1E−04	−20.8	<0.0001
PAR (1)	0.001	2.3E−04	4.39	<0.0001	0.001	2.1E−04	3.90	<0.0001
T_{air}	−0.928	0.095	−9.77	<0.0001	−0.609	0.090	−6.79	<0.0001
T_{air} (1)	−0.969	0.095	−10.2	<0.0001	−0.619	0.090	−6.89	<0.0001
VPD	3.113	0.466	6.67	<0.0001*	0.844	0.441	1.91	0.056
VPD (1)	2.438	0.464	5.26	<0.0001*	0.507	0.442	1.15	0.251
Pressure	−2.409	0.709	−3.40	0.001*	0.263	0.598	0.44	0.660
Pressure (1)	−2.033	0.708	−2.87	0.004*	0.709	0.596	1.19	0.234
VWC_{soils}	−0.683	0.409	−1.67	0.095	−1.375	0.460	−2.99	0.003
VWC_{soils} (1)	−0.697	0.405	−1.72	0.085	−1.363	0.453	−3.01	0.003
Rainfall	0.191	0.046	4.11	<0.0001	0.149	0.039	3.83	0.000
Burn × T_{air}	0.542	0.200	2.71	0.007	0.521	0.197	2.65	0.008
Burn × T_{air} (1)	0.620	0.199	3.11	0.002	0.532	0.196	2.71	0.007

MA(1) and MA(2) are estimated moving average terms at 1- and 2- period lags (½- and 1-h, respectively), and AR(1), AR(2), and AR(48) are estimated autoregressive terms at 1-, 2-, and 48- period lags (½-, 1-h, and 1 day, respectively); lagged values of independent variables are denoted similarly

PAR photosynthetically active radiation, T_{air} air temperature, *VPD* vapor pressure deficit, VWC_{soils} soil volumetric water content. The averaging period of this analysis is 0.5 h

* Significant difference between sites

mesic and xeric sites ($p < 0.02$), as well as a significant effect of windspeed and its half-hour lagged value ($p < 0.0001$), and a marginally significant effect of VWC ($p = 0.057$) in the mesic site. As PAR and windspeed increased, there was more release and as VWC decreased, there was more release. The Bonferroni correction indicated that only the effect of windspeed was significantly different by site, with a much stronger effect in the mesic site.

Discussion

Annual carbon dynamics

Differences in carbon dynamics varied by site, mainly due to the lower water holding capacity of the soils at the xeric site, which in turn altered the composition of the forest

Table 4 Parameter estimates from ARIMA model of ecosystem respiration (R_{eco}) by site

Parameter	Mesic site				Xeric site			
	Estimate	Standard error	t Value	Approx >|t|	Estimate	Standard error	t Value	Approx >|t|
Intercept	0.291	0.095	3.08	0.002	0.613	0.167	3.67	0.000
MA(1)	0.545	0.103	5.31	<0.0001	0.700	0.162	4.31	<0.0001
MA(2)	0.241	0.082	2.94	0.003	0.085	0.130	0.65	0.515
AR(1)	0.669	0.104	6.45	<0.0001	0.792	0.163	4.87	<0.0001
AR(2)	0.202	0.091	2.21	0.027	0.064	0.142	0.45	0.653
AR(48)	0.045	0.006	7.78	<0.0001	0.041	0.007	5.89	<0.0001
Burn	−0.367	0.379	−0.97	0.333	−0.749	0.410	−1.83	0.068
PAR	2.6E−06	1.1E−06	2.34	0.019	3.16E−06	1.0E−06	3.16	0.002
T_{air}	0.004	1.3E−04	29.74	<0.0001	0.004	1.2E−04	33.08	<0.0001
VPD	0.011	0.001	9.59	<0.0001	0.007	0.001	7.02	<0.0001
Pressure	−0.003	0.001	−2.84	0.005	−0.006	0.002	−3.70	0.000
Windspeed	0.004	0.001	5.98	<0.0001*	4.7E−04	0.001	0.80	0.421
Windspeed (1)	0.005	0.001	6.93	<0.0001*	0.001	0.001	1.46	0.145
VWC_{soils}	−0.001	4.0E−04	−1.91	0.057	6.2E−05	4.4E−04	0.14	0.888
Burn*T_{air}	−0.001	4.5E−04	−2.03	0.042	−0.001	3.7E−04	−4.03	<0.0001
Burn*VPD	−0.017	0.006	−2.76	0.006	−0.001	0.006	−0.14	0.887
Burn*Pressure	0.669	0.104	6.45	<0.0001	0.792	0.163	4.87	<0.0001

MA(1) and MA(2) are estimated moving average terms at 1- and 2- period lags (½- and 1-h, respectively), and AR(1), AR(2), and AR(48) are estimated autoregressive terms at 1-, 2-, and 48- period lags (½-, 1-h, and 1 day, respectively); lagged values of independent variables are denoted similarly

PAR photosynthetically active radiation, T_{air} air temperature, *VPD* vapor pressure deficit, WC_{soils} soil volumetric water content. The averaging period of this analysis is 0.5 h

* Significant difference between sites

and the ecosystem physiology (Addington et al. 2006; Ford et al. 2008). Addington et al. (2006), using the same sites as used here, reported that LAI varied from 0.22 to 0.39 m^2 m^{-2} for the xeric site, while the mesic site showed LAI almost three times larger (ranging from 0.65 to 1.1 m^2 m^{-2}). Ford et al. (2008) reported that greater water availability both due to greater water holding capacity of soils and enhanced access to the water table resulted in greater net primary production (NPP) in the mesic site. This contributed to a higher basal area, and above ground biomass was nearly 3-fold higher at the mesic site (Ford et al. 2008). The differences in soil VWC and LAI between sites controlled patterns in the carbon dynamics (NEE, Reco, GEE) reported in this study at both short-time scales (days-to-weeks) and at the annual scale in the absence of disturbance, i.e., fire.

When the C losses due to fire are not considered, the mesic site was a moderate carbon sink (-157.7 ± 25.1 g C m^{-2} $year^{-1}$), while the xeric site was carbon neutral (5.9 ± 32.8 g C m^{-2} $year^{-1}$) during the course of this study. Annual NEE rates reported here were also similar to those from mixed longleaf and slash pine flatwoods in North Central Florida also maintained with fire (Powell et al. 2008). Beringer et al. (2007) found

in Australia that an open woodland savanna had NEE exchange rates that were approximately double those found in our study, yet the ecosystem responded similarly in proportion to low intensity, high frequency fire.

After the application of prescribed fire, our sites transitioned from carbon sinks to sources. Prior to this prescribed burn, 2 years' worth of detritus accumulated from grasses and forbs (from the ground layer and overstory litter) and was largely released during the fires, resulting in fluxes on the order of 407.6 and 152.6 g C m^{-2} $year^{-1}$ for the mesic and xeric sites, respectively. These data point to: (a) the important and complex role that fires have in controlling C pools and fluxes in frequent fire systems, and (b) the need to understand the long term (decadal-scale) carbon balance over multiple fire cycles. Much of the past work has only evaluated C dynamics as a function of single stand replacement events, rather than multiple fire cycles (Wiedinmyer and Hurteau 2010). Our study provides information that begins to fill a gap in the scientific knowledge regarding the effects of frequent low intensity fire effects on the source/sink status of savanna ecosystems. In this study, we burned 2 years' of groundcover growth and detritus, and incorporated it in our annual NEE estimates. Yet, the understory and leaf litter biomass consumed by the fire was also part of NEE estimates in the time period between fires. As such, the effect of fire could be carbon neutral (when only considering all the production and consumption of fuels) when studying NEE over the 2-year fire cycle imposed on the sites.

While most of the environmental variables were similar at both sites, with the exception of soil moisture, there were some differences in carbon uptake and respiration responses. The higher respiration seen in the xeric site in June 2009 compared to July 2008 could be a result of an increase in heterotrophic respiration driven by fine root mortality following the fire. Since the uptake data showed no increase following fire, and primary producers would have to dedicate resources to rebuild aboveground organs, there could have been a compensatory decrease of fine root biomass to maintain optimal root-shoot ratios (Mokany et al. 2006). The higher uptake following fire in the mesic site was likely a result of increased nutrient availability (Wan et al. 2001) combined with the site's higher moisture availability that allowed the vegetation to recover before there was a reduction in root biomass.

Environmental drivers of ecosystem carbon dynamics

The time series model estimates indicated that there are complex relationships between ecosystem physiological activity and environmental drivers within each of these two sites. These relationships increase in complexity when fire is incorporated into the model analyses. While many effects interact, the models do not indicate complex lags in the system and all data series were stationary. On the other hand, ecological processes that experience disturbances from both internal and external forces may not be adequately described by ARIMA models (Gnauck et al. 2010). Moreover, the framework of the ARIMA models estimated here may not be adequate to capture low frequency, irregularly spaced disturbance (fire), since small perturbations to the system will be incorporated into residual error. Since flux data are influenced by inherent physical forces as well as disturbance, a model formulation which includes higher order statistical momenta, or multiresolution wavelet transformation may be appropriate to robustly account for multiple disturbances in longer time series. Nonetheless, this method presents a great improvement over data summarization techniques, allowing for an unbiased presentation of the complete record of flux data records in quantifying the drivers of carbon dynamics in these systems.

Our measurements of NEE were strongly affected by T_{air}, and this effect interacted with prescribed fire. While uptake increased with increasing T_{air}, this effect was significantly dampened during the 30 days post-fire, suggesting the combined effect of fire reducing understory leaf area and the respiring detritus pools. Nevertheless, uptake rates recovered quickly. We interpreted this effect as being caused by the rapid increase in understory LAI related to the fires occurring just prior to spring understory growth. In addition, during this same period we see candling and a new flush of pine needles from the canopy that also enhances the photosynthetic capacity of the system (Powell et al. 2008). These findings give support to our hypothesis that fire would not have a significant long lasting effect (<30 days) on longleaf pine ecosystem physiological activity as it relates to carbon dynamics since these systems have evolved with fire. This rapid recovery was similar to that observed in a mixed longleaf-slash pine ecosystem in North Central Florida (Lavoie et al. 2010). Once 30 days passed, the interactions between rates of recovery and seasonal warming during spring were difficult to separate, and due to the release of nitrogen caused by the fire, leaf area increased beyond those recorded prior to the fire. In a different study, Aubrey et al. (2012) showed that consecutive growing season canopy scorch manipulations resulted in a temporary reduction in ecosystem processes (lasting 1 month). Nonstructural carbohydrate reserves allowed for rapid recovery of the longleaf canopy which allowed for ecosystem processes to statistically remain the same for the year of the manipulations.

The effects of PAR, VPD, and atmospheric pressure varied significantly by site. PAR increased uptake in both sites, but more strongly so in the mesic site which could be associated with its greater LAI, soil VWC, and nutrient availability compared to the xeric site (Addington et al. 2006; Ford et al. 2008). VPD decreased uptake in both sites, but interestingly the effect was much stronger in the mesic site. The xeric site, which exhibits dry conditions for long periods of time may have evolved to maintain its physiological activity and hydrologic conductance as long as conditions do not reach critical levels (Addington et al. 2006).

R_{eco} was strongly affected by T_{air}, VPD and pressure, with these effects interacting with prescribed fire. While release increased with increasing T_{air}, this effect was significantly dampened in the 30 days post-fire. We attribute this decrease in R_{eco} to both decreases in autotrophic respiration caused by the removal of the understory vegetation during the fire, and in heterotrophic respiration through the removal of detritus pools (e.g., litter and coarse woody debris). Several studies have also shown the importance of elapsed time between fires, type and structure of vegetation, and the recovery rates of NEE and R_{eco} (Amiro et al. 2003; Trumbore 2006; Xu and Wan 2008). These interactions again show the complexity of ecosystem recovery from fire and the rapid onset of spring. For example, in the spring when temperatures increase, new needles flush, and soil VWC increases by rain events, all of which stimulate ecosystem respiration rates. There was significantly more release of carbon with increased windspeed in the mesic site, while in the xeric site the effect was not observed. We interpret this result as an increase of CO_2 storage below the canopy at the mesic site which has a slightly taller and denser canopy (Addington et al. 2006; Ford et al. 2008). This difference in canopy density allows for greater build up in CO_2 concentration during stable conditions and leads to larger CO_2 fluxes as a function of increased U. Soil VWC had a small, but significant effect in the mesic site's R_{eco}, where it led to smaller carbon loss with decreased VWC. Similar studies have also shown that in xeric conditions soil and ecosystem respiration rates were reduced with decreasing soil VWC, and that when wetting does occur significant increases in respiration rates are observed (Jarvis et al. 2007; Unger et al. 2012).

Even though most all EC studies measure atmospheric pressure, it is often used for unit conversions through the use of the ideal gas law, not as part of the statistical analyses of process rates and the abiotic drivers. We found that respiration rates were suppressed during periods of high pressure. Xu et al. (2014) found a similar association with atmospheric pressure constraining methane releases from landfills, while Kühne et al. (2012) found increased CO_2 diffusivity rates of soils with higher porosity. Given the high porosity of sandy soils at our sites, it is possible that conditions of higher static atmospheric pressures measurably reduced the diffusivity in the upper soil horizons. While more study is needed, this result may have an impact on how we measure soil efflux using surface soil chambers over highly porous soils.

Fire impacts on savanna-pine ecosystems

The productivity of these savanna-pine ecosystems shown here and elsewhere (Mitchell et al. 1999; Addington et al. 2006; Ford et al. 2008) are largely driven by available water. Hydrologic conditions prior to a fire, e.g., drought versus well-watered, determines how much of the carbon derived from the understory and leaf litter from mature trees is available for combustion. For example, one would expect that above average annual precipitation in years preceding the fire would result in larger C losses to fire. Drought after fire likely results in low productivity rates and longer times needed to accrue carbon due to the (previous) fire. As a consequence, knowledge of the hydrologic conditions, fire return interval, and the subsequent biomass accrual consumed during combustion over multiple fire cycles at the decadal is needed to fully understand savanna carbon source/sink trajectories which are very different than other systems that experience fire.

Many other ecosystems experience high intensity, low frequency, stand replacing wildfires that have a large impact on long-term C cycling (Amiro et al. 2003; Randerson et al. 2006; Rocha and Shaver 2011). Fire has an ability to re-organize the ecosystem structure and function in these ecosystems which can reset the trajectory of carbon dynamics. The intensity of this reorganization may be dependent on prior fire legacy and could have a long-lasting impact on the ecosystem (Harden et al. 2000). This is quite contrary to the effect of fire in longleaf pine systems reported here. Rather, the dynamics of high frequency and low intensity prescribed burns in longleaf systems maintain the forest structure and plant communities. For example, low intensity ground fires consume understory vegetation and litter as fuels and the overstory trees recover after being damaged from scorching (Beringer et al. 2007), in contrast to near entire removal of all above-ground carbon pools in high intensity fires. The relative effects of partial-to-total removal of carbon pools from differing ecosystems with varying fire frequency and intensity have only recently become the focus of studies in the context of ecosystem function (e.g., Litvak et al. 2003; Amiro et al. 2006; Nave et al. 2011). This is the first such study from longleaf pine forests contrasting work from high intensity, stand replacing fires.

Fire is still often viewed as a disturbance that can re-set the whole ecosystem, driving the community composition, structure and function toward new trajectories. These trajectories are often described as a non-linear path incorporating severity and frequency of perturbations and their legacies, mechanisms of recruitment and establishment and time (Chapin et al. 2009). Here, fire does re-set this system through: (1) the removal of litter, (2) maintaining the existing plant diversity (Kirkman et al. 2004; Glitzenstein et al. 2012), and (3) limiting the migration and recruitment of ruderal species. In addition, fire

has limited to no effect on canopy mortality rate due to the low intensity of the fire. Hence, fire maintains the existing structure, function, and carbon process of the ecosystem. Fire exclusion on the other hand, fosters the establishment of *Quercus sp*., that alter fuel characteristics such that areas dominated by oaks are often resistant to subsequent fires (Glitzenstein et al. 1995). This resets this ecosystem on an entirely different trajectory with different stability (Scheffer 2009; Carpenter 2003). To restore the function of longleaf pine ecosystems after such a transition is difficult, costly, and time consuming (Provencher et al. 2001). Our study establishes a foundation for understanding the linkages between ecosystem resiliency and fire in longleaf pine dominated systems; however we acknowledge that our study was limited to one prescribed fire and 1 year of study. To strengthen the idea of longleaf pines resiliency to fire longer-term study will need to be pursued.

Conclusions

This study develops an understanding of the complex interactions between abiotic and biotic factors controlling longleaf pine ecosystem carbon dynamics under controlled fire regimes and provides a proof of concept for using analytical time series models with EC data. Fire was associated with the immediate release of carbon to the atmosphere through combustion and had a role in altering the sink/source capacity of these two ecosystems during the short period of this study. Analysis of the non-linear behavior of fluxes pre- and post-fire indicated that fire has a role in NEE and R_{eco} processes for 30 days following fire. Although there is a complex interaction between fire, ecosystem phenology (new needle production) and changing environmental conditions, this study provides a method for improving our understanding of fire's direct effects on longleaf pine ecosystems. There are still many uncertainties associated with how these interactions change with fluctuating environmental conditions and whether this system is a carbon sink, source, or neutral over long time scales (Sierra et al. 2009). Our study does suggest, however, that if climate in the southeastern United States experience greater periods of drought longleaf pine ecosystems may reduce their ability to sequester carbon. In closing we argue that fire is a cyclical event and must be studied within ecosystems for multiple fire events to truly understand the complex interactions that occur between soil water availability, fire, environment, and structure and function of longleaf ecosystems.

Acknowledgments This research has been funded by U. Alabama and the Joseph Jones Ecological Research Center (JJERC). Authors also wish to acknowledge the superlative logistical support of the JJERC, especially J Bradley, B Shelton, and M Mazzacavaallo. HW Loescher acknowledges the National Science Foundation (DBI-0752017). We would also like to thank the two previous reviewers who helped increase the clarity of this manuscript through their suggestion on an early version of this paper. This paper would not have taken shape if it were not the guidance, lifetime work, and for many a conversation with J. Franklin.

Appendix

See Tables 5 and 6.

Table 5 Distribution of parameters from daytime net ecosystem exchange (NEE_{day}) bootstrap simulations

Site	Year	Month	α (μmol CO_2 μmol quanta^{-1})				P_{max} (μmol CO_2 m^{-2} s^{-1})				R_d (μmol CO_2 m^{-2} s^{-1})			
			Estim. param.	LCL	Median	UCL	Estim. param.	LCL	Median	UCL	Estim. param.	LCL	Median	UCL
Mesic	2008	7	−0.057	−0.083	−0.057	−0.039	−20.074	−21.843	−20.132	−18.432	7.704	5.982	7.696	9.524
		8	−0.064	−0.091	−0.063	−0.046	−18.958	−21.025	−18.980	−17.245	7.670	6.045	7.657	9.536
		9	−0.035	−0.049	−0.035	−0.026	−21.318	−23.365	−21.373	−19.737	4.527	3.324	4.527	5.932
		10	−0.066	−0.174	−0.065	−0.037	−16.924	−20.998	−16.939	−15.027	6.029	3.629	5.896	10.964
		11	−0.055	−0.113	−0.054	−0.030	−12.773	−15.280	−12.894	−11.306	4.447	2.550	4.399	7.287
		12	−0.039	−0.051	−0.039	−0.030	−13.197	−14.755	−13.259	−12.202	2.462	1.904	2.492	3.141
	2009	1	−0.024	−0.040	−0.024	−0.015	−9.537	−11.867	−9.634	−8.212	1.733	0.952	1.757	2.529
		2	−0.018	−0.024	−0.018	−0.014	−14.051	−16.249	−14.131	−12.795	2.458	1.941	2.561	3.215
		3	−0.014	−0.021	−0.014	−0.010	−16.411	−21.005	−16.497	−14.408	1.912	1.026	1.915	2.889
		4	−0.036	−0.054	−0.036	−0.025	−16.151	−18.123	−16.139	−14.861	4.474	3.167	4.404	6.659
		5	−0.051	−0.066	−0.051	−0.039	−22.003	−23.452	−22.088	−20.734	5.672	4.409	5.652	6.971
		6	−0.065	−0.107	−0.064	−0.044	−23.035	−26.122	−23.007	−20.983	8.016	5.814	7.938	11.600
Xeric	2008	7	−0.036	−0.061	−0.036	−0.022	−17.674	−20.237	−17.895	−16.105	4.704	3.332	4.746	6.611
		8	−0.044	−0.069	−0.045	−0.030	−19.898	−22.475	−20.058	−17.878	5.291	3.692	5.331	7.654
		9	−0.028	−0.038	−0.027	−0.020	−20.702	−23.888	−20.845	−18.650	3.451	2.375	3.409	4.766
		10	−0.020	−0.042	−0.020	−0.010	−10.499	−13.840	−10.760	−8.896	1.580	0.326	1.645	3.498
		11	−0.011	−0.022	−0.011	−0.005	−7.669	−15.710	−7.772	−6.300	0.679	−0.027	0.681	1.509
		12	−0.015	−0.033	−0.015	−0.008	−8.470	−14.241	−8.625	−6.918	1.451	0.748	1.475	2.383
	2009	1	−0.014	−0.036	−0.015	−0.007	−6.583	−10.349	−6.746	−5.435	2.197	1.559	2.233	3.075
		2	−0.011	−0.024	−0.011	−0.006	−6.787	−8.729	−6.905	−5.837	1.926	1.188	1.899	3.013
		3	−0.016	−0.025	−0.016	−0.011	−8.183	−9.632	−8.223	−7.186	2.914	2.325	2.936	3.585
		4	−0.031	−0.046	−0.032	−0.023	−12.659	−13.940	−12.742	−11.721	4.302	3.499	4.329	5.466
		5	−0.056	−0.076	−0.056	−0.043	−22.115	−23.741	−22.167	−20.775	6.871	5.657	6.828	8.556

Table 5 continued

Site	Year	Month	α (μmol CO_2 μmol quanta^{-1})				P_{max} (μmol CO_2 m^{-2} s^{-1})				R_d (μmol CO_2 m^{-2} s^{-1})			
			Estim. param.	LCL	Median	UCL	Estim. param.	LCL	Median	UCL	Estim. param.	LCL	Median	UCL
		6	−0.058	−0.084	−0.060	−0.045	−19.345	−21.412	−19.477	−18.020	6.862	5.561	7.011	8.934

LCL lower limit of 95 % confidence region, *UCL* upper limit of 95 % confidence region, α is the apparent quantum efficiency (−μmol CO_2 μmol quanta^{-1}), R_d is ecosystem respiration (μmol CO_2 m^{-2} s^{-1}), and P_{max} is the maximum ecosystem CO_2 uptake rate

Table 6 Distribution of parameters from nighttime net ecosystem exchange (NEE_{night}) bootstrap simulations

Site	Year	Month	R_0 (μmol CO_2 m^{-2} s^{-1})				b (μmol CO_2 m^{-2} s^{-1})			
			Estim. param.	LCL	Median	UCL	Estim. param.	LCL	Median	UCL
Mesic	2008	9	2.213	1.243	2.244	3.501	0.035	0.013	0.034	0.061
		11	1.164	0.912	1.164	1.476	0.057	0.036	0.057	0.076
		12	1.122	0.952	1.129	1.311	0.054	0.042	0.054	0.065
	2009	1	1.141	0.975	1.136	1.299	0.048	0.039	0.048	0.057
		2	1.102	0.748	1.097	1.519	0.051	0.027	0.050	0.080
		3	1.318	0.952	1.318	1.681	0.051	0.035	0.051	0.072
		4	1.020	0.711	1.011	1.343	0.069	0.052	0.070	0.089
		5	2.928	1.614	3.018	4.457	0.026	0.005	0.025	0.055
	Annual		1.171	1.062	1.171	1.278	0.062	0.058	0.062	0.066
Xeric	2008	9	1.449	0.674	1.448	2.657	0.052	0.024	0.052	0.085
		10	1.478	1.123	1.480	1.880	0.039	0.024	0.039	0.055
		11	1.073	0.667	1.085	1.430	0.069	0.046	0.068	0.100
		12	1.351	1.161	1.355	1.554	0.030	0.021	0.030	0.040
	2009	1	1.077	0.914	1.077	1.255	0.068	0.056	0.068	0.078
		2	1.067	0.892	1.059	1.265	0.040	0.029	0.040	0.051
		3	1.284	0.896	1.236	1.548	0.052	0.042	0.054	0.069
		4	1.391	1.010	1.371	1.828	0.058	0.043	0.058	0.075
	Annual		1.304	1.206	1.302	1.420	0.055	0.051	0.055	0.059

LCL lower limit of 95 % confidence region, *UCL* upper limit of 95 % confidence region. R_0 is the base respiration rate when air temperature is 0 °C and b is an empirical coefficient

References

Abrahamson WG, Hartnett DC (1990) Pine flatwoods and dry prairies. In: Myers RL, Ewel JJ (eds) Ecosystems of Florida. University Press of Florida, Gainesville, pp 103–148

Addington RN, Donavan LA, Mitchell RJ, Vose JM, Pecot SD, Jack SB, Hacke UG, Sperry JS, Oren R (2006) Adjustments in hydraulic architecture of *Pinus palustris* maintain similar stomatal conductance in xeric and mesic habitats. Plant Cell Environ 29:535–545

Amiro BD, MacPherson JI, Desjardins RL, Chen JM, Liu J (2003) Post-fire carbon dioxide fluxes in the western Canadian boreal forest: evidence from towers, aircraft and remote sensing. Agric Forest Meteorol. doi:10.1016/j.bbr.2011.03.031

Amiro BD, Orchansky AL, Barr AG, Black TA, Chambers SD, Chapin FS III, Goulden ML, Litvak M, Liu HP, McCaughey JH, McMillan A, Randerson JT (2006) The effect of post-fire stand age on the boreal forest energy balance. Agric Forest Meteorol 140:41–50

Aubrey DP, Mortazavi B, O'Brien JJ, McGee JD, Hendricks JJ, Kuehn KA, Teskey RO, Mitchell RJ (2012) Influence of repeated canopy scorching on soil CO2 efflux. Forest Ecol Manag 282:142–148

Balshi MS, McGuire AD, Duffy P, Flannigan M, Kicklighter DW, Melillo J (2009) Vulnerability of carbon storage in North American boreal forests to wildfires during the 21st century. Global Change Biol 15(6):1491–1510

Beringer J, Hutley LB, Tapper NJ, Cernusak LA (2007) Savanna fires and their impact on net ecosystem productivity in North Australia. Global Change Biol 13:990–1004

Bond WJ, Woodward FI, Midgley GF (2005) The global distribution of ecosystems in a world without Fire. New Phytol 165:525–537

Bond-Lamberty B, Peckham SD, Ahl DE, Gower ST (2007) Fire as the dominant driver of central Canadian boreal forest carbon balance. Nature 450:89–92

Box GEP, Gwilym M, Jenkins G, Reinsel C (1994) Time series analysis: forecasting and control, 3rd edn. Prentice Hall, NJ

Brocklebank JC, Dickey A (2003) SAS for forecasting time series, 2nd edn. SAS Institute Inc., Cary, NC

Carpenter SR (2003) Regime shifts in lake ecosystems: pattern and variation. Ecology Institute, Oldendorf/Luhe

Chapin III FS, Folke C, Kofinas GP (2009) A framework for understanding change. In: Chapin III FS, Kofinas GP, Folke C (eds) Principles of ecosystem stewardship. Springer, New York

Christensen NL (1981) Fire regimes in Southeastern ecosystems. In: Mooney HA, Bonnicksen TM, Christensen NL, Lotan JE, Reiners WA (eds) Fire regimes and ecosystem properties. USDA, Washington, DC. For. Serv. Gen. Tech. Rep. GTR-WO-26. pp 112–136

Clement R (1999). http://www.geos.ed.ac.uk/abs/research/micromet/EdiRe

DC NC (2002) Monthly station normals of temperature, precipitation and heating and cooling degree-days 1971–2000. National Climatic Data Center, Asheville, NC

Dickey DA, Fuller WA (1979) Distribution of the estimators for autoregressive time series with a unit root. J Am Stat Assoc 74(366):427–431

Foken T, Leclerc MY (2004) Methods and limitations in validation of footprint models. Agric Forest Meteorol 127(3–4):223–234

Ford CR, Mitchell RJ, Teskey RO (2008) Water table depth affects productivity, water use, and the response to nitrogen addition in a savanna system. Can J Forest Res 38:2118–2127

Girod CM, Hurtt GC, Frolking S, Aber JD, King AW (2007) The tension between fire risk and carbon storage: evaluating US carbon and fire management strategies through ecosystem models. Earth Interact 11:1–33

Glitzenstein JS, Platt WJ, Streng DR (1995) Effects of fire regime and habitat on tree dynamics in north Florida longleaf pine savannas. Ecol Monogr 65(4):441–476

Glitzenstein JS, Streng DR, Masters RE, Robertson KM, Herman SM (2012) Fire-frequency effects on vegetation in north Florida pinelands: another look at the long-term Stoddard fire research plots at tall timbers research station. Forest Ecol Manag 264:197–209

Gnauck A, Lee BL, Feugo JDL, Luther B (2010) The role of statistics for long term ecological research. In: Müller F, Baessler C, Schubert H, Klotz S (eds) Long term ecological research: between theory and practice. Springer, Berlin

Goebel PC, Palik BJ, Kirkman LK, Drew MB, West L et al (2001) Forest ecosystems of a Lower Gulf Coastal Plain landscape: multifactor classification and analysis. J Torrey Bot Soc 128:47–75

Grace J, San Jose J, Meir P, Miranda HS, Montes RA (2006) Productivity and carbon fluxes of tropical savannas. J Biogeogr 33:387–400

Harden JW, Trumbore SE, Stocks BJ, Hirsch A, Gower ST, O'Neill KP, Kasischke ES (2000) The role of fire in the boreal carbon budget. Global Change Biol 6:174–184

IPCC (2014) Climate change 2014: impacts, adaptation, and vulnerability. In: Working Group II contribution to the IPCC 5th assessment, Cambridge University Press, Cambridge

Jarvis P, Rey A, Petsikos C, Wingate L, Rayment M, Pereira J, Banaza J, David J, Miglietta F, Borghetti M, Manca G, Valentini R (2007) Drying and wetting of Mediterranean soils stimulates decomposition and carbon dioxide emission: the "Birch effect". Tree Physiol 27:929–940

Kirkman LK, Goebel PC, Palik BJ, West LT (2004) Predicting plant species diversity in a longleaf pine landscape. EcoScience 11:80–93

Kruger FJ (1983) Plant community diversity and dynamics in relation to fire. Ecological studies. In: Kruger FJ, Mitchell DT, Jarvis JUM (eds) Mediterranean-type ecosystems: the role of nutrients. Springer, New York, pp 446–472

Kühne A, Schack-Kichner H, Hildebrand EE (2012) Gas diffusivity in soils compared to ideal isotropic porous media. J Plant Nutr Sci 175:34–45. doi:10.1002/jpin.201000438

Lavoie M, Starr G, Mack MC, Martin TA, Gholz HL (2010) Impact of prescribed fire on understory biomass production and nutrient availability in a naturally-regenerated longleaf pine-slash pine forest in north central Florida. Nat Areas J 30(1):82–94

Litvak ME, Miller S, Wofsy SC, Goulden ML (2003) Effect of stand age on whole ecosystem CO_2 exchange. J Geophy Res 108(D3):8225. doi:10.1029/2001JD000854. Special section: comparison of carbon exchange between Boreal Black Spruce Forests and the atmosphere for a wildfire age sequence (FIRE-EXB)

Lloyd J, Taylor JA (1994) On the temperature dependence of soil respiration. Funct Ecol 8:315–323

Loescher HW, Munger JW (2006) Preface to special section on new approaches to quantifying exchanges of carbon and energy across a range of scales. J Geophys Res Atmos 111:D14S91. doi:10.1029/2006JD007135

Loescher HW, Law BE, Mahrt L, Hollinger DY, Campbell J, Wofsy SC (2006a). Uncertainties in, and interpretation of, carbon flux estimates using the eddy covariance technique. J Geophys Res Atmos 111:D21S90. doi:10.1029/2005JD006932

Loescher HW, Starr G, Martin TA, Binford M, Gholz HL (2006b) The effect of daytime circulations on eddy covariance carbon dioxide flux measurements over a *Pinus elliottii* canopy. J Appl Meteorol Clim 45:1127–1140

Martin PH, Nabuurs GJ, Aubinet M, Karjalainen T, Vine EL, Kinsman J, Heath L (2001) Carbon sinks in temperate forests. Annu Rev Energ Environ 26:435–465

Massman WJ (2000) A simple method for estimating frequency response corrections for eddy covariance systems. Agric Forest Meteorol 104:185–198

Massman WJ (2004) Toward an ozone standard to protect vegetation based on effective dose: a review of deposition resistances and a possible metric. Atm Environ 38(15):2323–2337

Mitchell RJ, Kirkman LK, Pecot SD, Wilson CA, Palik BJ, Boring LR (1999) Patterns and controls of ecosystem function in longleaf pine-wiregrass savannas: I. aboveground net primary productivity. Can J Forest Res 29:743–751

Mitchell RJ, Hiers JK, O'Brien JJ, Starr G (2009) Ecological forestry in the Southeast: understanding the ecology of fuels. J For 107(8):391–397

Mitchell RJ, Liu Y, O'Brien JJ, Elliott KJ, G Starr, Maniat CF, Hiers JK (2014) Future climate and fire interactions in the Southeastern region of the United States. Forest Ecol Manag. doi:10.1016/j.foreco.2013.12.003

Mokany K, Raison R, Prokushkin AS (2006) Critical analysis of root: shoot ratios in terrestrial biomes. Glob Change Biol 12(1):84–96

Nave L, Gough CM, Maurer KD, Bohrer C, Hardiman B, Le Moine J, Munoz AB, Nadelhoffer K, Sparks JP, Strahm BD, Vogel CS, Curtis PS (2011) Disturbance and the resilience of coupled carbon and nitrogen cycling in a north temperature forest. J Geophys Res 116. doi:10.1029/2011/JG001758

Ocheltree TW, Loescher HW (2007) Design of the AmeriFlux portable eddy covariance system and uncertainty analysis of carbon measurements. J Atmos Ocean Technol 24(8):1389–1406

Ottmar RD, Sandberg DV, Riccardi CL, Prichard SJ (2007) An overview of the fuel characteristic classification system (FCCS): quantifying, classifying, and creating fuelbeds for resource planning. Can J Forest Res 37:1–11

Powell TL, Gholz HL, Clark KL, Starr G, Cropper WP Jr, Martin TA (2008) Carbon exchange of a mature, naturally regenerated pine forest in north Florida. Global Change Biol 14:2523–2538

Provencher L, Herring BJ, Gordon DR, Rodgers HL, Galley KE, Tanner GW, Hardesty JL, Brennan LA (2001) Effects of hardwood reduction techniques on longleaf pine sandhill vegetation in northwest Florida. Restor Ecol 9:13–27

Randerson JT, Chapin FS III, Harden JW, Neff JC, Harmon ME (2002) Net ecosystem production: a comprehensive measure of net carbon accumulation by ecosystems. Ecol Appl 12:937–947

Randerson JT, Liu H, Flanner MG, Chambers SD, Jin Y, Hess PG, Pfister G, Mack MC, Treseder KK, Welp LR, Chapin FS, Harden JW, Goulden ML, Lyons E, Neff JC, Schuur EAG, Zender CS (2006) The influence of boreal forest fire on climate warming. Science 314:1130–1132

Rocha AV, Shaver GR (2011) Burn severity influences postfire CO_2 exchange in arctic tundra. Ecol Appl 21(2):477–489

Ruimy A, Jarvis PG, Baldocchi DD, Saugier B (1995) CO_2 fluxes over plant canopies and solar radiation: a review. Adv Ecol Res 26:1–68

Ryan MC, Williams M (2011) How does fire intensity and frequency affect miombo woodland tree populations and biomass? Ecol Appl 21:48–60

Scheffer M (2009) Critical transitions in nature and society. Princeton University Press, Princeton

Sierra CA, Loescher HW, Harmon ME, Richardson AD, Hollinger DY, Perakis SS (2009) Interannual variation of carbon fluxes from a tropical, a temperate, and a boreal evergreen forest: the role of forest dynamics and climate. Ecology 90:2711–2723

Trumbore S (2006) Carbon respired by terrestrial ecosystems: recent progress and challenges. Global Change Biol 12(2):141–153

Unger S, Máguas C, Pereira JS, David TS, Werner C (2012) Interpreting post-drought rewetting effects on soil and ecosystem carbon dynamics in a Mediterranean oak savannah. Agric Forest Meteorol 154–155:9–18

Wan S, Hui D, Luo Y (2001) Fire effects on nitrogen pools and dynamics in terrestrial ecosystems: a meta-analysis. Ecol Appl 11(5):1349–1365

Way AG (2006) Burned to be wild: Herbert Stoddard and the roots of ecological conservation in the southern longleaf pine forest. Environ Hist 11:500–526

Whelan A, Mitchell RJ, Staudhammer CL, Starr G (2013) The cyclic occurrence of fire and its role in carbon dynamics along an edaphic moisture gradient in longleaf pine ecosystems. PLoS One 8(1):e54045. doi:10.1371/journal.pone.00540

Wiedinmyer C, Hurteau MD (2010) Prescribed burning as a means of reducing carbon emissions in the Western United States. Environ Sci Technol 44:1926–1932

Wiedinmyer C, Neff JC (2007) Estimates of CO_2 from fires in the United States: implications for carbon management. Carbon Balanc Manag. doi:10.1186/1750-0680-2-10

Xu, W, Wan S (2008) Water- and plant-mediated responses of soil respiration to topography, fire, and nitrogen fertilization in a semiarid grassland in northern China. Soil Bio Biochem. doi:10.1016/j.bbr.2011.03.031

Xu L, Lin X, Amen J, Welding K, McDermitt D (2014) Impact of changes in barometric pressure on landfill methane emission. Global Biogeochem Cy. doi:10.1002/2013GB004571